

TRIGGERED STAR FORMATION INSIDE THE SHELL OF A WOLF-RAYET BUBBLE AS THE ORIGIN OF THE SOLAR SYSTEM

VIKRAM V. DWARKADAS

Astronomy and Astrophysics, University of Chicago, 5640 S Ellis Ave, ERC 569, Chicago, IL 60637

NICOLAS DAUPHAS

Origins Laboratory, Department of the Geophysical Sciences and Enrico Fermi Institute, The University of Chicago, 5734 South Ellis Avenue, Chicago IL 60637

BRADLEY MEYER

Department of Physics and Astronomy, Clemson University, Clemson, SC, 29634-0978, USA.

PETER BOYAJIAN

Astronomy and Astrophysics, University of Chicago, 5640 S Ellis Ave, ERC 569, Chicago, IL 60637

MICHAEL BOJAZI

Department of Physics and Astronomy, Clemson University, Clemson, SC, 29634-0978, USA.

ABSTRACT

A critical constraint on solar system formation is the high $^{26}\text{Al}/^{27}\text{Al}$ abundance ratio of 5×10^{-5} at the time of formation, which was about 17 times higher than the average Galactic ratio, while the $^{60}\text{Fe}/^{56}\text{Fe}$ value was about 2×10^{-8} , lower than the Galactic value. This challenges the assumption that a nearby supernova was responsible for the injection of these short-lived radionuclides into the early solar system. We show that this conundrum can be resolved if the Solar System was formed by triggered star formation at the edge of a Wolf-Rayet (W-R) bubble. Aluminium-26 is produced during the evolution of the massive star, released in the wind during the W-R phase, and condenses into dust grains that are seen around W-R stars. The dust grains survive passage through the reverse shock and the low density shocked wind, reach the dense shell swept-up by the bubble, detach from the decelerated wind and are injected into the shell. Some portions of this shell subsequently collapses to form the dense cores that give rise to solar-type systems. The subsequent aspherical supernova does not inject appreciable amounts of ^{60}Fe into the proto-solar-system, thus accounting for the observed low abundance of ^{60}Fe . We discuss the details of various processes within the model and conclude that it is a viable model that can explain the initial abundances of ^{26}Al and ^{60}Fe . We estimate that 1-16% of all Sun-like stars could have formed in such a setting of triggered star formation in the shell of a WR bubble.

Keywords: Astrochemistry, Meteoroids, Solar System: Formation

vikram@oddjob.uchicago.edu

dauphas@uchicago.edu

mbradle@g.clemson.edu

peterhaigboyajian@gmail.com

mbojazi@g.clemson.edu

1. INTRODUCTION

The discovery and subsequent characterization of extrasolar planetary systems has shed new light on the origin and peculiarities of the solar system. Astronomical observations offer clues about the grand architecture of planetary systems. They cannot provide, however, access to the intricate details that the study of meteorites offers. One important constraint on models of solar system formation comes from measurements of the abundances of now extinct short-lived radionuclides, whose past presence is inferred from isotopic variations in their decay products. Isotopic abundances in meteorites provide insight into the makeup of the cloud material from which the solar system formed. They can be used as tracers of the stellar processes that were involved in the formation of the solar system, and of galactic chemical evolution up until the time of solar system formation.

More than 60 years ago, Urey (1955) speculated about the possible role of ^{26}Al as a heat source in planetary bodies. It was not until 1976, however, that Lee et al. (1976) demonstrated the presence of this radioactive nuclide in meteorites at a high level. The high abundance of ^{26}Al ($^{26}\text{Al}/^{27}\text{Al} \sim 5 \times 10^{-5}$) at solar system birth (Lee et al. 1976; MacPherson et al. 1995; Jacobsen et al. 2008) can be compared to expectations derived from modeling the chemical evolution of the Galaxy (Meyer & Clayton 2000; Wasserburg et al. 2006; Huss et al. 2009), or γ -ray observations (Diehl et al. 2006), which give a maximum $^{26}\text{Al}/^{27}\text{Al}$ ratio of $\sim 3 \times 10^{-6}$ (Tang & Dauphas 2012). Aluminium-26 in meteorites is in too high abundance to be accounted for by long-term chemical evolution of the Galaxy or early solar system particle irradiation (Marhas et al. 2002; Duprat & Tatischeff 2007). Instead, ^{26}Al must have been directly injected by a nearby source (see §2). Such sources can include supernovae (Cameron & Truran 1977; Meyer & Clayton 2000), stellar winds from massive stars (Arnould et al. 1997; Diehl et al. 2006; Arnould et al. 2006; Gaidos et al. 2009; Gounelle & Meynet 2012; Young 2014; Tang & Dauphas 2015; Young 2016), or winds from an AGB-star (Wasserburg et al. 2006). The latter is unlikely, because of the remote probability of finding an evolved star at the time and place of solar system formation (Kastner & Myers 1994). Recent calculations by Wasserburg et al. (2017) have shown that it is unlikely that an AGB star could simultaneously account for the abundances of ^{26}Al , ^{60}Fe , ^{182}Hf and ^{107}Pd . Aluminium-26 is mainly produced by hot bottom burning in stars $\gtrsim 5M_{\odot}$, which produce too little ^{182}Hf and ^{107}Pd . The latter are mainly products of neutron capture processes in stars $\lesssim 5M_{\odot}$. A small window of AGB star masses between 4-5.5 M_{\odot} could be made

to work, but this requires that hot bottom burning in these stars was stronger than was assumed in their calculations, and/or an additional neutron source was present.

One way to test whether supernovae or stellar winds from massive stars are the source is to examine ^{60}Fe ($t_{1/2}=2.6$ Myr) (Wasserburg et al. 1998). This radioactive nuclide is produced mostly by neutron capture in the inner part of massive stars, whereas ^{26}Al is produced in the external regions (Limongi & Chieffi 2006). If a supernova injected ^{26}Al , one would expect copious amounts of ^{60}Fe to also be present.

The formation of refractory Ca, Al-rich inclusions (CAIs) in meteorites marks time zero in early solar system chronology (Dauphas & Chaussidon 2011). To better constrain the $^{60}\text{Fe}/^{56}\text{Fe}$ ratio at CAI formation, many studies in the early 2000's analyzed chondrites using Secondary Ion Mass Spectrometry (SIMS) techniques, and reported high $^{60}\text{Fe}/^{56}\text{Fe}$ ratios of $\sim ^{60}\text{Fe}/^{56}\text{Fe} = 6 \times 10^{-7}$. For reference, the expected $^{60}\text{Fe}/^{56}\text{Fe}$ ratio in the interstellar medium (ISM) 4.5 Ga from γ -ray observations (Wang et al. 2007) is $\sim 3 \times 10^{-7}$ without accounting for isolation from fresh nucleosynthetic input before solar system formation (Tang & Dauphas 2012). The SIMS results were later shown to suffer from statistical artifacts, leading Telus et al. (2012) to revise downward the initial $^{60}\text{Fe}/^{56}\text{Fe}$ ratios that had been previously reported.

The high initial $^{60}\text{Fe}/^{56}\text{Fe}$ ratios inferred from *in situ* measurements of chondritic components contradicted lower estimates obtained from measurements of bulk rocks and components of achondrites. This led to speculations that ^{60}Fe was heterogeneously distributed in the protoplanetary disk, with chondrites and achondrites characterized by high and low $^{60}\text{Fe}/^{56}\text{Fe}$ ratios, respectively (Sugiura et al. 2006; Quitté et al. 2010, 2011).

The issue of the abundance and distribution of ^{60}Fe in meteorites was addressed by Tang and Dauphas (Tang & Dauphas 2012, 2015). Using Multi Collector Inductively Coupled Plasma Mass Spectrometry (MC-ICPMS), these authors measured various components from chondrites Semarkona (LL3.0), NWA 5717 (un-grouped 3.05) and Gujba (CBa), as well as bulk rocks and mineral separates from HED and angrite achondrites. They showed that in these objects, the initial $^{60}\text{Fe}/^{56}\text{Fe}$ ratio was low, corresponding to an initial value at the formation of CAIs of $11.57 \pm 2.6 \times 10^{-9}$. They also measured the $^{58}\text{Fe}/^{56}\text{Fe}$ ratio and found that it was constant between chondrites and achondrites, thus ruling out a heterogeneous distribution of ^{60}Fe as collateral isotopic anomalies on ^{58}Fe would be expected. Some SIMS studies have continued to report higher ratios but the data do not define clear isochrones (Mishra et al. 2010; Mishra & Chaussidon

2012; Marhas & Mishra 2012; Mishra & Chaussidon 2014; Mishra & Goswami 2014; Telus et al. 2016). Furthermore, recent measurements using the technique of Resonant Ionization Mass Spectrometry (RIMS; (Trappitsch et al. 2017; Boehnke et al. 2017)) have called into question the existence of the ^{60}Ni excesses measured by SIMS. *The weight of evidence at the present time thus favors a low uniform initial $^{60}\text{Fe}/^{56}\text{Fe}$ ratio at solar system formation (Tang & Dauphas 2012, 2015).*

The low initial $^{60}\text{Fe}/^{56}\text{Fe}$ ratio may be consistent with derivation from background abundances in the Galaxy with no compelling need to invoke late injection from a nearby star (Tang & Dauphas 2012). Iron-60 is a secondary radioactive isotope and ^{56}Fe is a primary isotope with respect to nucleosynthesis. To first order, models of galactic chemical evolution find that the ratio of the abundance of a primary nuclide (proportional to time t) to a secondary nuclide (proportional to $t \times \tau$, since it depends on the primary isotope, as well as on its half-life τ), should be roughly constant in time over Galactic history (Huss et al. 2009). This indicates that the ISM ratio at the time of the Sun’s birth was probably near $\sim 3 \times 10^{-7}$, the current value inferred from γ -ray observations. This value, however, is an average over all phases of the ISM. The ^{60}Fe ejected from supernovae predominantly goes into hot material that then takes some tens of millions of years to cool down to a phase that can undergo new star formation. We expect that this delay reduces the $^{60}\text{Fe}/^{56}\text{Fe}$ ratio to the low value inferred from chondrites.

The fundamental challenge in reconciling the early solar system abundances of ^{26}Al and ^{60}Fe is thus to understand how to incorporate freshly made ^{26}Al without adding too much ^{60}Fe . Adjusting the timescale between nucleosynthesis and solar system formation does not help because ^{26}Al has a shorter half-life than ^{60}Fe , so any delay would cause the $^{26}\text{Al}/^{60}\text{Fe}$ ratio to decrease, making the problem worse. Some possible scenarios that have been suggested to explain the high $^{26}\text{Al}/^{60}\text{Fe}$ ratio of the early solar system include (1) supernova explosion with fallback of the inner layers, so that only ^{26}Al is efficiently ejected while ^{60}Fe is trapped in the stellar remnant (Meyer & Clayton 2000), but this is unlikely because one would need to have fallback that extends to external regions in the star (a cutoff in the C/O-burning layer) to prevent ^{60}Fe from escaping (Takigawa et al. 2008), (2) interaction of a supernova with an already formed cloud core, so that only the outer layers are efficiently injected while the inner layers are deflected (Gritschneider et al. 2012), and (3) ejection of ^{26}Al in the winds of one or several massive stars (Arnould et al. 1997; Diehl et al. 2006; Arnould et al. 2006; Gaidos et al. 2009; Tatischeff et al. 2010; Gounelle & Meynet 2012;

Young 2014; Tang & Dauphas 2015; Young 2016). The last scenario is the most appealing because it could be a natural outcome of the presence of one or several Wolf-Rayet (W-R) stars, which shed their masses through winds rich in ^{26}Al , whereas ^{60}Fe is ejected at a later time following supernova explosion. The W-R winds expanding out into the surrounding medium would have carved wind-blown bubbles in molecular cloud material, and would have enriched the bubbles in ^{26}Al , which would have later been incorporated in the molecular cloud core that formed the solar system.

In this contribution, we take this idea a step further and suggest that our solar system was born inside the shell of a Wolf-Rayet wind bubble. Using a combination of semi-analytic calculations, astronomical observations, and numerical modeling, we show that a single massive star would produce enough ^{26}Al to enrich the entire solar system, that this ^{26}Al would be incorporated into the dense shell surrounding the wind-blown bubble, and that molecular cores within the dense shell would later collapse to form the solar protoplanetary nebula. In §2 we discuss the sources and yields of ^{26}Al . §3 discusses the formation and evolution of W-R bubbles, and the production of ^{26}Al in these bubbles. Triggered star formation at the periphery of these bubbles is the topic of §4. The transport of ^{26}Al is the subject of §5, including condensation of ^{26}Al onto dust grains and injection of ^{26}Al into the dense shell. The subsequent SN explosion, and whether the shell would be contaminated further by explosive ^{60}Fe , is discussed in §6. The timing of formation of the proto-solar disk is discussed in §7. Finally, further discussion of our model and conclusions are dealt with in §8.

2. SOURCES OF ^{26}Al

Aluminium-26 is a radioactive nuclide, with a half-life of about 0.7 Myr. The radioactive decay of ^{26}Al leads to the emission of 1.8 MeV gamma-rays. More than 20 years ago, Prantzos & Diehl (1995), discussing Comptel data, suggested that “massive stars embedded in the spiral arms dominate the 1.8 MeV sky image”. In 1999, Knödlseher (1999) showed from an analysis of Comptel data that the 1.8 MeV gamma-ray line was closely correlated with the 53 GHz free-free emission in the Galaxy. The free-free emission arises from the ionized interstellar medium. They argued that this could be understood if massive stars are the source of ^{26}Al , as had already been suggested by Prantzos & Diehl (1996). Knödlseher (1999) showed that the correlation was also strong with other tracers of the young stellar population.

The distribution of ^{26}Al in the Galaxy closely traces the distribution of very massive stars, making W-R stars and core-collapse SNe the primary candidates for ^{26}Al production. The former are stars with initial mass

$\gtrsim 25 M_{\odot}$, which have lost their H and possibly He envelopes. Many authors have suggested that stellar winds from massive stars, could be the source of ^{26}Al in the early solar system (Arnoult et al. 1997; Diehl et al. 2006; Arnould et al. 2006; Gounelle & Meynet 2012; Young 2014; Tang & Dauphas 2015; Young 2016). Aluminium-26 has been seen towards star forming regions such as Vela (Oberlack et al. 1994) and Cygnus (Martin et al. 2010). Voss et al. (2010) used a census of the most massive stars in Orion to compute the stellar content in the region, followed by the ejection of ^{26}Al from these stars. They found good agreement between their model and the ^{26}Al signal in the Orion region. Diehl et al. (2010) detected a significant ^{26}Al signal, $> 5\sigma$ above the background, from the Scorpius-Centaurus region. In a study of the Carina region using INTEGRAL data, Voss et al. (2012) found that the ^{26}Al signal could not be accounted for by supernovae alone, and the fraction of ^{26}Al ejected in W-R stars is high.

2.1. Aluminium-26 in Massive Stars

Aluminium-26 is mainly produced in stars in the main sequence H-burning phase, by the $^{25}\text{Mg}(p, \gamma)^{26}\text{Al}$ proton-capture reaction (Limongi & Chieffi 2006). The conversion starts at the beginning of the main sequence, and comes to completion within the H-burning lifetime. The ^{26}Al production reaches a maximum shortly after the onset of H burning, after which it β decays into ^{26}Mg , on a timescale of order 10^6 yr. Since production still continues, the ^{26}Al abundance decrease is slower than it would be for pure β decay, but it does not reach a stable state. After the exhaustion of core H burning, the ^{26}Al is found in the He core and in the H left behind by the receding core. This would be mainly lost during the explosion, but because massive stars have dredge ups and lose significant amounts of mass, the ^{26}Al can be expelled in the stellar wind. In stars that become W-R stars, there are no significant dredge-up episodes, ^{26}Al is preserved in the He core, and ejected mainly through mass loss which can reach deep into the interior (Limongi & Chieffi 2006). Thus, although it is produced in the early stages, it is only in the post-main-sequence phases, especially in W-R stars, that most of the ^{26}Al is expelled through wind loss, making W-R stars one of the primary producers of ^{26}Al into the interstellar medium. Aluminium-26 is also produced in explosive nucleosynthesis, but as we will show later this is inconsequential in our model.

In order to quantify the production of ^{26}Al in massive stars, we have compiled computations of the ^{26}Al production from several groups (Langer et al. 1995; Limongi & Chieffi 2006; Palacios et al. 2005; Ekström et al. 2012; Georgy et al. 2012, 2013). Most

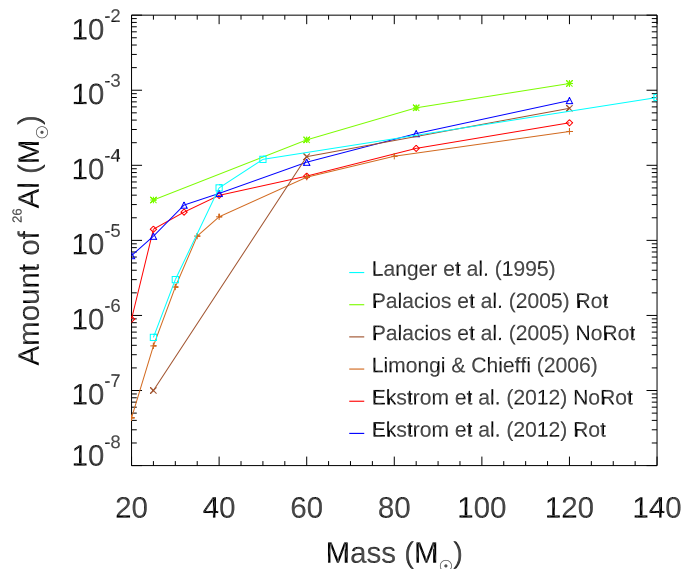


Figure 1. Amount of ^{26}Al lost from massive stars with mass $> 20 M_{\odot}$. References cited: Ekström et al. (2012): no rotation, $Z=.014$; Ekström et al. (2012): $V/V_c = .4$, $Z=.014$; Limongi & Chieffi (2006) only wind: no rotation; Palacios et al. (2005): $V_o = 0 \text{ km s}^{-1}$, $Z=0.02$; Palacios et al. (2005): $V_o = 300 \text{ km s}^{-1}$, $Z=0.02$; Langer et al. (1995) Wind, $Z=.02$. [V_c =critical rotation velocity (expressed in km s^{-1} , or as a fraction of critical velocity); V_o = surface rotation velocity].

of the models provide the total ^{26}Al yield at the end of the evolution of the star. The later calculations (Ekström et al. 2012; Georgy et al. 2012, 2013), which take into account updated solar metallicity (0.014), stellar rotation and improved mass-loss rates, provide the ^{26}Al yield throughout the stellar evolution history, thus allowing us to evaluate not only the total yield but also when ^{26}Al was lost in the wind, and thus take the decay of ^{26}Al into account. In Figure 1 we have plotted the ^{26}Al yields from stars with initial mass $\geq 20 M_{\odot}$. In general, a single massive Wolf-Rayet (W-R) star provides at least $10^{-5} M_{\odot}$ of ^{26}Al . The more massive the star, the higher the ^{26}Al yield. The spread in the ^{26}Al amount produced is due to differences in the nuclear reaction rates, which by itself can produce a difference of up to a factor of 3 in the yield (Iliadis et al. 2011), as well as differences intrinsic to the stellar model physics such as mixing, mass-loss rates, rotation velocities, and magnetic fields. The ^{60}Fe yield from the wind itself is negligible, as the ^{60}Fe is primarily produced in these massive stars in the He convective shell, and is not ejected by the stellar wind (Limongi & Chieffi 2006).

3. WOLF-RAYET BUBBLES

W-R stars form the post-main-sequence phase of massive O-type main sequence stars. The physical proper-

ties and plausible evolutionary scenarios of W-R stars are detailed in Crowther (2007). Although their evolutionary sequence is by no means well understood, it is generally accepted that they form the final phase of massive stars $> 25M_{\odot}$ before they core-collapse to form SNe. These stars have radiatively driven winds with terminal velocities of $1000\text{-}2000 \text{ km s}^{-1}$ (Crowther 2001), and mass-loss rates of order 10^{-7} to $10^{-5} M_{\odot} \text{ yr}^{-1}$ in the W-R phase. The high surface temperature of these hot stars ($> 30,000 \text{ K}$) results in a large number of ionizing photons - the UV ionizing flux is of order $10^{49} \text{ photons s}^{-1}$ (Crowther 2007).

In Figure 2, we show the evolution of the wind mass-loss rate in a $40 M_{\odot}$ non-rotating star (Ekström et al. 2012). The mass-loss rate is lowest in the main-sequence phase (up to $\sim 4.5 \times 10^5$ years), increases in the subsequent He-burning red supergiant phase, and then drops somewhat in the W-R phase as the star loses its H envelope. The figure also shows the ^{26}Al loss rate (the ^{26}Al emitted per year) in the wind. Note that this also increases in the post-main-sequence phases, and essentially follows the mass-loss.

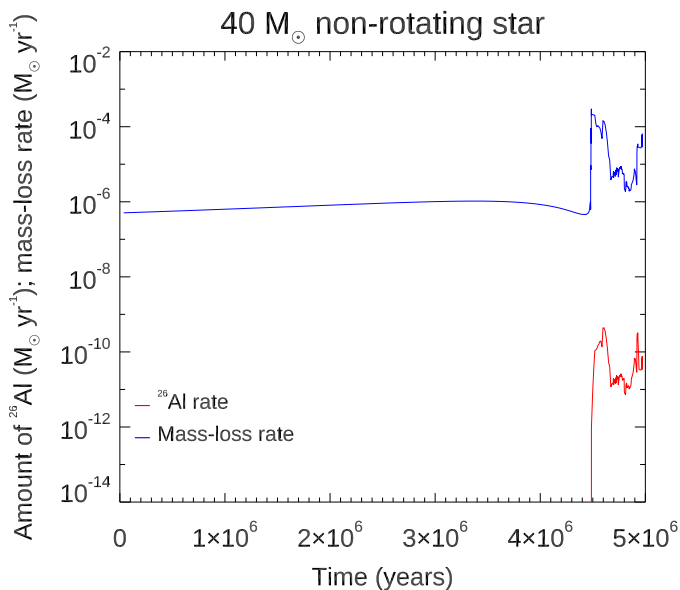


Figure 2. The evolution of the wind mass-loss rate (blue) in a non-rotating $40 M_{\odot}$ star. The parameters are taken from the stellar models of Ekström et al. (2012). The mass-loss rate is approximately steady or slowly increasing throughout the main-sequence phase, but increases dramatically in the post-main-sequence red supergiant and W-R phases. The figure shows (in red) the amount of ^{26}Al lost per year via the wind.

The combined action of the supersonic winds and ionizing radiation results in the formation of photo-ionized wind-blown bubbles around the stars, consisting of a low-density interior surrounded by a high-density shell.

The nature of wind-driven bubbles was first elucidated by Weaver et al. (1977). Going outwards in radius, one can identify 5 distinct regions: (1) a freely expanding wind, (2) a shocked wind region, (3) a photoionized region, (4) a thin dense shell, and (5) the external medium. A reverse or wind termination shock separates the freely expanding wind from the shocked wind. The external boundary is generally a radiative shock, which compresses the swept-up material to form a thin, dense shell, enclosed between the radiative shock and a contact discontinuity on the inside.

Models of wind-blown bubbles incorporating both the photo-ionizing effects of the hot stars and the gas dynamics have been computed by Toalá & Arthur (2011) and Dwarkadas & Rosenberg (2013). In Figure 3 we show the evolution of a W-R bubble around a $40 M_{\odot}$ star. Most of the volume is occupied by the shocked wind region (blue in the figure) which has a low density and high temperature. The ionizing photons create the photo-ionized region which extends beyond the wind-blown region in this particular case due to the high number of ionizing photons. The thin shell is susceptible to various hydrodynamical instabilities that disrupt the smooth spherical symmetry, causing the surface to be corrugated, and leading to variations in the shell density.

The parameters of the bubble that are important towards our investigation are the radius of the bubble and the swept-up mass. The theory of wind-blown bubbles was first derived by Weaver et al. (1977). The radius of the bubble can be written as:

$$R_b = 0.76 \left[\frac{L_w}{\rho_a} \right]^{1/5} t^{3/5} \text{ cm} \quad (1)$$

where $L_w = 0.5 \dot{M} v_w^2$, which has dimensions of energy over time, is called the mechanical wind luminosity, ρ_a is the ambient density and t is the age, all in cgs units. The massive stars that we are considering here have lifetimes of 3.7-5 million years depending on their initial mass. The lifetime of these stars is a complicated function of mass and metallicity, because the mass-loss from the star, which strongly affects its lifetime, is a function of the metallicity. Schaerer (1998) gives the lifetime of solar metallicity stars as a function of mass as

$$\log \tau_{total} = 9.986 - 3.496 \log(M) + 0.8942 \log(M)^2 \quad (2)$$

where τ_{total} is the lifetime in years and M is the star's initial mass in solar mass units. For a $40 M_{\odot}$ star this gives 4.8 million years.

The wind mass-loss rates and wind velocities vary over the stellar types, and continually over the evolution, and are an even more complicated function of the mass, lu-

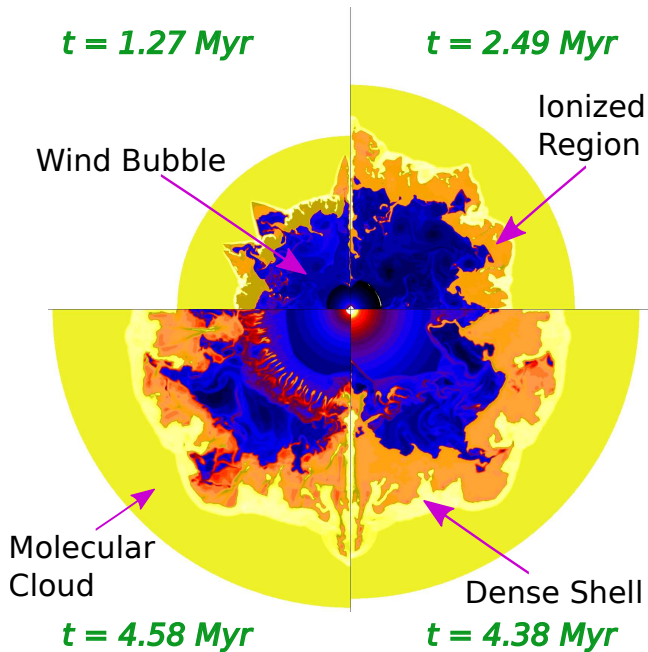


Figure 3. Wind-blown bubble around a Wolf-Rayet Star. The figure shows the density at 4 epochs in the evolution of a wind-blown bubble around a $40 M_{\odot}$ star, starting clockwise from top left, at 1.27, 2.49, 4.38 and 4.58 Myr. (The parameters for this simulation are taken from [van Marle et al. \(2005\)](#), with mass-loss rates somewhat different from those shown in Figure 2). The blue region is the wind-driven bubble, which is separated from the dense shell (light yellow) by the golden ionized region. The shell is unstable to several instabilities, related to both the hydrodynamics and the ionization front, which cause fragmentation and the formation of dense filaments and clumps. The wind-driven bubble in this case reaches the dense swept-up shell only during the Wolf-Rayet phase.

minosity, and Eddington parameter of the star. However, a representative mass-loss rate of $10^{-6} M_{\odot} \text{ yr}^{-1}$ and wind velocity of 1000 km s^{-1} in the main sequence phase gives a value of $L_w > 10^{35} \text{ g cm}^2 \text{ s}^{-3}$ in the main sequence phase, increasing perhaps up to $10^{36} \text{ g cm}^2 \text{ s}^{-3}$ in the W-R phase.

The swept-up mass depends on how far the bubble shell can expand, and the surrounding density. Wind-driven nebulae around W-R stars are found to be around 3-40 pc in size ([Cappa 2006](#)). The surrounding ISM density is usually around a few, rarely exceeding 10 cm^{-3} ([Cappa et al. 2003](#)). If we assume a value of 10 cm^{-3} in equation 1 and the value of L_w appropriate for the main-sequence phase (since that is where the star spends 90% of its life), we get a radius $R_b = 27.5 \text{ pc}$ for a $40 M_{\odot}$ star for example. Lower densities will give larger radii. Furthermore, if the surrounding pressure is high, the bubble pressure comes into pressure equilibrium with the surroundings in less than the stellar lifetime, after which the bubble stalls.

The mass of the dense shell is the mass swept up by the bubble shock front up to that radius, and therefore

the mass of molecular cloud material up to that radius. Values of the density and volume of the thin shell, and therefore the swept-up mass, are difficult quantities to infer both theoretically and observationally. From those that have been estimated, we find that observed swept-up shell masses have a maximum value of around $1000 M_{\odot}$ ([Cappa et al. 2003](#)), with a small number exceeding this value. The swept-up shell mass in our calculations is therefore taken to be $1000 M_{\odot}$.

3.1. ^{26}Al from Massive Stars compared to the Early solar System

How do the ^{26}Al amounts emitted by massive stars (§2.1) compare with the amount of ^{26}Al required to explain the observed value in meteorites? The initial concentration of ^{26}Al at the time of formation of the solar system can be calculated taking the recommended abundances for the proto-solar system from [Lodders \(2003\)](#), which gives $N(\text{H})=2.431 \times 10^{10}$, $N(\text{He})=2.343 \times 10^9$, and $N(^{27}\text{Al})=8.41 \times 10^4$. Using the ratio of $^{26}\text{Al} / ^{27}\text{Al} = 5 \times 10^{-5}$ ([Lee et al. 1976](#)), we can write the mass of ^{26}Al per unit solar mass (the ‘concentration’ of ^{26}Al) at solar system formation as

$$C_{^{26}\text{Al}, \text{pss}} = \frac{5 \times 10^{-5} \times 8.41 \times 10^4 \times 26}{2.431 \times 10^{10} + 2.343 \times 10^9 \times 4} = 3.25 \times 10^{-9} \quad (3)$$

This is consistent with the value given in [Gounelle & Meynet \(2012\)](#).

We assume that the solar system is formed by the collapse of dense material within the dense shell swept-up by the W-R bubble. Some fraction η of the ^{26}Al produced is mixed throughout the dense shell, giving a resulting concentration that is equal to or greater than that computed above. Since ^{26}Al is not produced in the W-R stage, but is mixed in with the shell during this stage, we allow for the decay of the ^{26}Al in the W-R phase, which lasts for a maximum period $t_d = 300,000$ years (we do not consider smaller W-R periods because given the half-life of ~ 0.7 Myr, a smaller W-R phase will not lead to significant decay and thus further bolster our arguments). We use a half-life of ^{26}Al of 7.16×10^5 years ([Rightmire et al. 1959](#); [Samworth et al. 1972](#)). After ^{26}Al is all mixed in, we assume that some fraction of the shell collapses to form a dense molecular core that will give rise to the proto-solar nebula.

The ^{26}Al concentration after mixing with the dense shell is given as:

$$C_{^{26}\text{Al}, \text{bub}} = \frac{\eta M_{^{26}\text{Al}}}{M_{\text{shell}}} e^{-t_d \ln(2)/t_{1/2}} \quad (4)$$

The swept-up shell mass in our calculations has been assumed to be $1000 M_{\odot}$ as mentioned above, which is on the upper end of observed shell masses. The concentra-

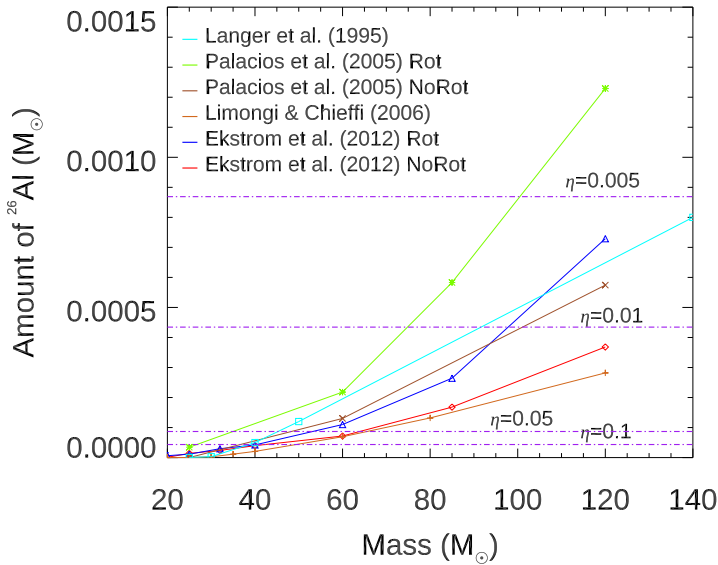


Figure 4. The amount of ^{26}Al emitted is taken from Figure 1. The dashed purple lines indicate the minimum mass of ^{26}Al required for different values of the fraction η , to give the initial solar system concentration. Where these thresholds cross the curves for the various ^{26}Al amounts gives the minimum mass star needed to fulfill the requirements.

tion will be inversely proportional to the shell mass, so it can always be scaled to different masses. Lower masses are not a problem, as this just makes it easier to achieve the required concentration. Higher shell masses would make it more difficult for the required ^{26}Al concentration to be achieved, but observations show a much higher mass would be quite unusual.

Figure 4 shows the amount of ^{26}Al produced, and the values of η that satisfy the equality $C_{^{26}\text{Al},\text{bub}} = C_{^{26}\text{Al},\text{pss}}$, for a decay period of 300,000 years. Since all the ^{26}Al is not expected to mix with the dense shell, a maximum value of $\eta = 0.1$ is assumed, as well as a minimum value $\eta = 0.005$ below which no reasonable solution is found. It can be seen that a range of solutions exists, depending on which stellar models and values of ^{26}Al production one considers. If one assumes an efficiency of 10% to be reasonable, then stars above around $50 M_{\odot}$ could produce the required ^{26}Al concentration. Lower efficiencies require higher mass stars as expected; an efficiency of 1% can only be matched for some models with stars of mass $> 100 M_{\odot}$, and cannot be achieved at all in most models. The newer stellar models produce less ^{26}Al , and thus require higher efficiencies. The efficiency also depends on the mass of the shell. If the shell mass is higher, the efficiency will be correspondingly lower for a given ^{26}Al mass. Most W-R shell masses though do not exceed a thousand M_{\odot} (Cappa et al. 2003).

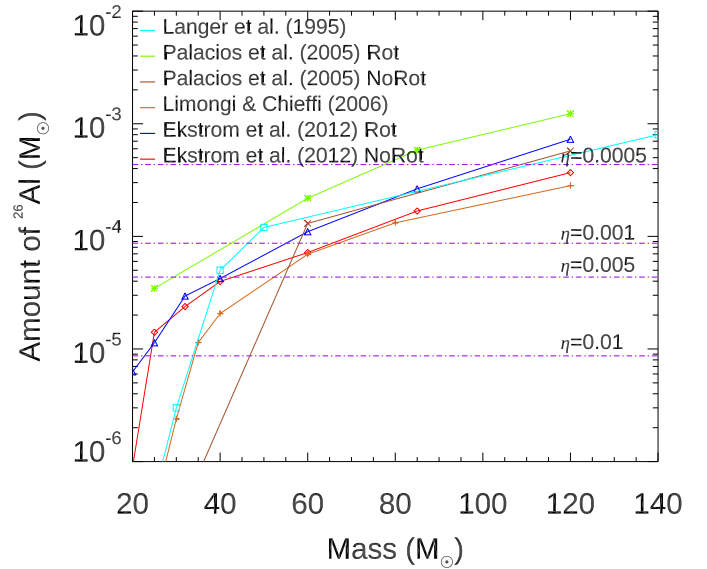


Figure 5. Similar to Figure 4, but for a minimum solar mass nebula. Now it is clear that even demanding a low 1% efficiency, most models suggest that all W-R stars would be able to satisfy the initial ^{26}Al requirements.

Another possibility exists which considerably eases the issue of adequate ^{26}Al concentration in the early solar system. While the ^{26}Al concentration is determined for the meteorites, it is uncertain whether the same amount was present in the Sun. Indeed, some early formed refractory condensates found in meteorites and known as FUN (with fractionation and unidentified nuclear isotope anomalies) calcium-aluminium inclusions, lack ^{26}Al , raising the possibility that ^{26}Al was heterogeneously distributed in the early solar system and thus the abundance of ^{26}Al inferred from non-FUN CAIs may not be relevant to the solar system as a whole. It could be that this concentration is representative of the protoplanetary disk around the Sun but not the star itself. One could thus assume that the ^{26}Al is only present in a minimum mass solar nebula (Weidenschilling 1977), with mass about $0.01 M_{\odot}$. In that case, equation 3 would be multiplied by 0.01, thus reducing the concentration to $C_{^{26}\text{Al},\text{min}} = 3.25 \times 10^{-11}$. This would make it much simpler for the requirements to be satisfied. Even assuming only 1% of ^{26}Al is injected into the dense shell, we find that in many scenarios, almost all stars which make ^{26}Al , above about $25 M_{\odot}$ depending on which models are adopted, would be enough to satisfy the ^{26}Al requirement (Figure 5).

4. STAR FORMATION WITHIN WOLF-RAYET BUBBLES

Observations of molecular and infrared emission from dense neutral clouds adjacent to OB associations led

Elmegreen & Lada (1977) to postulate that ionization fronts, and the associated shock fronts, trigger star formation. This was especially seen to occur near the interface between HII regions (regions of ionized H) and dense clouds, where the ionization front is expected to be located. Massive stars formed in this manner then evolve and give rise to HII regions surrounding them, which leads to another generation of star formation. Thus the process could lead to sequential star formation. This is generally now referred to as the “collect and collapse” mechanism for star formation, because the ionization front collects the material between it and the shock front, leading to an increase in density, which causes the cloud material to collapse and form stars. These conditions are exactly the ones prevalent at the edge of wind-blown bubbles, where the ionization front is being driven into the dense shell, leading to formation of cloud cores and a new generation of stars. The timescale for triggering is proportional to $(G\rho_{sh})^{-1/2}$, where G is the Gravitational constant and ρ_{sh} is the density of the collapsing material (dense shell). Generally, the most unstable wavelength is comparable to the shell thickness, as would be expected for thin shell instabilities. Analytic studies of the process were completed by Whitworth et al. (1994b,a). Simulations (Hosokawa & Inutsuka 2005, 2006b,a) have shown that shells driven into molecular clouds do have time to collapse and form stars, and that triggered star formation does work.

Another somewhat similar mechanism where the ionization front ablates the cloud, generating a shock that compresses the cloud, causing clumps to collapse, is the radiation-driven implosion model, elaborated on by Lefloch & Lazareff (1994) as a way to explain bright rimmed clouds and cometary globules. This operates on a shorter timescale compared to the previous mechanism, and also in a smaller spatial region. The actual mechanism is hard to distinguish and not always clear. Walch et al. (2015) suggest that a hybrid mechanism, that combines elements of both processes, may be at work in the HII region RCW120. Recent reviews of both observational and theoretical aspects of triggered star formation can be found in Elmegreen (2011) and Walch (2014).

Observational evidence for triggered star formation has been found at the boundaries of wind-bubbles around massive O and B stars (Deharveng et al. 2003, 2005; Zavagno et al. 2007; Watson et al. 2009; Brand et al. 2011). Further evidence arises from statistical correlation of young stellar objects with wind bubbles. Kendrew et al. (2012) investigated infrared bubbles in the Milky Way project and found that two-thirds of massive young stellar objects were located within a projected distance of 2 bubble radii, and about 1 in 5

found between 0.8 and 1.6 bubble radii. Furthermore, as the bubble radius increased (and thus the swept-up shell mass increases) they found a statistically significant increase in the overdensity of massive young sources in the region of the bubble rim. Also pertinent to the current discussion, molecular cores undergoing gravitational collapse due to external pressure from the surrounding gas have been found around W-R star HD 211853 (Liu et al. 2012b). The cores have been estimated as being from 100,000 to greater than a million years old. Thus, both observational and theoretical considerations suggest a high probability of triggered star formation at the boundaries of wind-blown bubbles, where suitable conditions are both predicted and observed.

5. TRANSPORT OF ^{26}Al

Another important ingredient needed to evaluate the plausibility of the W-R injection scenario is the mechanism for injection of ^{26}Al from the wind into the dense shell. One aspect that has been conspicuously absent is a discussion of the mechanism of mixing of the ^{26}Al from the hot wind into the cold dense shell. Gounelle & Meynet (2012) attributed it to turbulent mixing without giving further details. Young (2014, 2016) assumes mixing from winds to clouds without providing details of the process. Gaidos et al. (2009) suggested that dust grains were responsible for the delivery of ^{26}Al from W-R winds into the molecular cloud, where they were stopped by the high density clouds. However they did not investigate the properties of the dust grains seen around W-R stars. Tatischeff et al. (2010) realized that mixing of the hot winds into the colder and denser material was a difficult problem, but refuted the arguments of Gaidos et al. (2009) on the basis that (1) grains (assumed to be about $0.01\ \mu\text{m}$) would be stopped before they reached the dense shell and (2) that the mean velocity for the emitting ^{26}Al nuclei of about $150\ \text{km s}^{-1}$, derived from the broadening of the 1.8 MeV line seen with RHESSI and INTEGRAL gamma-ray satellites, was too low for them to have survived sputtering at the reverse shock. Instead they formulated a model where the mixing is due to instabilities in the bow shock region created by a runaway W-R star that moves relative to the center of mass of the W-R bubble. These instabilities tend to mix the W-R wind material with the surrounding material, which is most likely material ejected during the star’s prior evolution, mixed in perhaps with some pre-existing material.

The mixing of fast hot material (such as from the winds) with slower cold material (as in the dense shell), has been more thoroughly studied in the context of injection by a SN shock wave, and insight can be gained from those results. Boss (2006) and Boss & Keiser (2013) have shown that the injection efficiency due to hydro-

dynamic mixing between a SN shock wave and the collapsing cores is small, of order a few percent. In their model the mixing occurs late in the SN evolution, when it has reached the radiative stage and the SN shock has slowed down to $< 100 \text{ km s}^{-1}$. This requires the SN to be several pc away from the initial solar system so that the shock can slow down from its initial velocity of thousands of km s^{-1} . The SPH simulations of [Goswami & Vanhala \(2000\)](#) also show that shock velocities between 20 and 45 km s^{-1} are required to trigger collapse. However their calculations with a variable adiabatic exponent γ appear to suggest that the hot shocked gas is still unable to penetrate the cold cores due to buoyancy and entropy effects, further complicating the issue. An alternate model by [Ouellette et al. \(2007\)](#) proposed a SN that was much closer (0.3 pc) to the proto-solar nebula. This model though did not account for the ionizing radiation from the progenitor star ([Tatischeff et al. 2010](#)). [McKee et al. \(1984\)](#) showed that massive stars that core-collapse as SNe could clear out large regions of space around them due to their ionizing radiation. Thus the disk would be adversely affected even before the star collapsed to form a SN, and it is not clear how viable this model is.

The W-R wind velocity substantially exceeds the SN shock velocity discussed above of 100 km s^{-1} . W-R winds also have a much lower density than SN ejecta, since the density is proportional to the mass-loss rate and inversely to the velocity. The efficiency of mixing in winds will therefore be further reduced. Furthermore, winds sweeping past high-density cores will lead to shearing at the edges of the cores, leading to the growth of Kelvin-Helmholtz instabilities at the interface, and essentially stripping material away. Some material will be mixed in, but it will be a very small fraction. Hydrodynamic mixing does not appear a viable mechanism in this scenario. We suggest instead that ^{26}Al condenses onto grains that serve as injection vectors into the bubble shell, a conclusion that was also reached by [Gaidos et al. \(2009\)](#) for stellar wind injection and [Ouellette et al. \(2010\)](#) for SN injection.

5.1. Dust in Wolf-Rayet Bubbles

Infrared emission, indicative of dust, has been seen in carbon-rich W-R (WC) stars since 1972 ([Allen et al. 1972](#)). Even early on, it was realized that circumstellar dust emission was present mostly around the late carbon-rich sub-types of W-R stars, WC8-WC10 stars ([Williams et al. 1987](#)), as well as a WN10 (N-rich W-R) star. The clearest manifestation of dust however was the observation of a ‘pinwheel nebula’ around WR 140 ([Tuthill et al. 1999](#)). In this case it was clear that the presence of interacting winds due to a companion star was responsible for the formation of dust. This was

followed by the discovery of another pinwheel nebula around the star WR 98a, further solidifying the binary connection. It is conjectured, although not conclusively shown, that only WC stars out of all the W-R stars are capable of producing dust, either steadily or episodically ([Williams 2002](#)). Even though the number of stars is small, dust seen in WC stars is important because the absolute rate of dust production is found to be high ($\sim 10^{-6} M_{\odot} \text{ yr}^{-1}$ of dust) ([Marchenko & Moffat 2007](#)), and a few percent of the total wind mass. Analysis of the IR emission showed that dust forms close in to the star.

Modelling the IR emission from WR 112, [Marchenko et al. \(2002\)](#) suggested a grain size of $0.49 \pm 0.11 \mu\text{m}$. This is consistent with the results from [Chiar & Tielens \(2001\)](#) who inferred grain sizes of around $1 \mu\text{m}$ from ISO spectroscopy and analysis of the dust around the stars WR 118, WR 112 and WR 104. Dust grain sizes of around $0.3\text{-}2 \mu\text{m}$ are also inferred from modelling the dust around WR 95 and WR 106 ([Rajagopal et al. 2007](#)). Thus it appears that dust grains formed in WR bubbles have sizes predominantly around $1 \mu\text{m}$. It has been now shown that dust can be formed around WC stars, Luminous Blue Variable (LBV) stars, and possibly WN stars ([Rajagopal et al. 2007](#)), although the latter is questionable. There is, however, no doubt that dust can be formed around carbon-rich WC stars, and LBV stars which may transition to W-R at a later stage.

5.1.1. Condensation of ^{26}Al into Dust Grains

Given the presence of dust in WC stars, we address further the question of ^{26}Al transport. One of the arguments made by [Tatischeff et al. \(2010\)](#), that grains would not be able to survive, is negated by the presence of mainly large μm size grains in W-R winds, which we show later do manage to survive. Sputtering at the reverse shock does not appear to be a problem in the low density wind for the large grains. Regarding the low expansion velocity indicated by the line broadening, this is indicative of the bulk velocity of the grains and unrelated to the issue of grain destruction. As we show later, in our model ^{26}Al takes only about 20,000 years to travel from the star to the dense shell, after which its velocity would decrease considerably before coming to a complete stop. This is much smaller than the lifetime of 0.7 Myr, thus at any given time we would expect most of the ^{26}Al to be expanding at a low velocity in the dense shell rather than at the wind velocities. The Doppler velocity and therefore linewidth would be representative of the average bulk velocity, and therefore be dominated by the low velocity ^{26}Al decaying in the cavity walls. In fact such a scenario was already envisioned by [Diehl et al. \(2010\)](#), who explained the low

expansion velocity by postulating that ^{26}Al was being slowed down, on a scale of about 10pc, by interacting with the walls of pre-existing wind-blown cavities in the region. Our work shows how this scenario would work in practice.

One important question is whether ^{26}Al would condense into dust grains. Equilibrium calculations (Fedkin et al. 2010) suggest that would be the case. In general, in stars such as LBVs, the outer layers would condense to give aluminium oxides. In the carbon-rich WC stars, AlN would be the dominant Al condensing phase. One must also not neglect the fact that most dust-producing WC stars are in a binary system, and the companion is generally an O-type MS star, thus suggesting that H may still be present in the system, leading to the formation of hydrocarbons. In the final, oxygen-rich phase of W-R stars (WO), it would be the oxides that would dominate again. Although the calculations by Fedkin et al. (2010) are equilibrium calculations, and consider only stars up to $25 M_{\odot}$, they do suggest that most of the ^{26}Al would condense into dust grains. Ouellette et al. (2010) also discuss this issue in detail, providing arguments drawn from theory and astronomical observations to support the idea that the condensation efficiency of ^{26}Al is around 10%.

5.1.2. Injection of ^{26}Al into the Solar nebula

Once the ^{26}Al condenses into dust grains, this dust must travel several pc from the vicinity of the star out to the dense shell. Grains can be destroyed by thermal sputtering at the reverse shock of the wind blown bubble. According to Draine & Salpeter (1979), the lifetime against thermal sputtering in the hot gas is:

$$t_{\text{sput}} \approx 2 \times 10^4 \left[\frac{n_H}{\text{cm}^{-3}} \right]^{-1} \left[\frac{a}{0.01 \mu\text{m}} \right] \text{ yr} \quad (5)$$

where n_H is the number density within the bubble, and a is the size of the dust grain. For typical wind bubbles evolving in the interstellar medium, bubble densities are of order $n_H = 10^{-2} \text{ cm}^{-3}$. Using a grain size of $a = 1 \mu\text{m}$, the lifetime is 10^8 years, almost two orders of magnitude greater than the stellar lifetime. The interior density of the bubble goes as (Weaver et al. 1977; Dwarkadas 2007) $\rho_{\text{am}}^{3/5}$, so that even if the external density were as high as 10^3 cm^{-3} (which is highly unlikely over the entire bubble expansion), the bubble internal density is about 0.6, and the lifetime against sputtering still exceeds a million years. This could be a sizable fraction of the star's lifetime, and certainly exceeds the duration of the W-R phase of any massive star. Furthermore, calculations of C dust destruction in SNe have shown that C grains are the most resistant amongst all species to sputtering (Nozawa et al. 2006; Biscaro & Cherchneff 2016) and are therefore most likely to survive sputter-

ing at shocks. Thus over the entire relevant parameter range, thermal sputtering can be considered negligible for the large size dust grains found in W-R bubbles.

The stopping distance (d) of a grain with size a and grain density ρ_g in the interstellar bubble with density ρ_b is given by $d = \rho_g / \rho_b \times a$ (Spitzer 1978). For μm size grains with grain density 2 g cm^{-3} in a bubble with internal density $n_H = 10^{-2} \text{ cm}^{-3}$, the stopping distance is found to be of order 3000 pc, far larger than the size of the bubble in the high density molecular cloud. Even for a large interior density of $n_H = 1 \text{ cm}^{-3}$, which is highly unlikely, the stopping distance of 30pc is comparable to the size of the bubble. Even if we take into account the fact that this formula may overestimate the range (Ragot 2002), it is still clear that for most reasonable parameters the dust grains will survive passage through the bubble. Indeed, Marchenko et al. (2002) find observationally in the case of WR 112 that about 20% of the grains may be able to reach the interstellar medium.

The dust grains are carried by the W-R wind out to the dense shell. Once the wind reaches the dense shell, it is strongly decelerated, but the grains will detach from the wind and continue moving forward into the dense shell. The stopping distance of the grains will now be reduced. Since the shell density is $10^4 - 10^5$ times higher than the density in the bubble interior, the stopping distance correspondingly reduces from pc to 10's to 100's of AU. Following Ouellette et al. (2007), the time taken for the dust to lose half its initial velocity is $t_{1/2} = 16 \rho_g a / (9 \rho_b v_w)$, which is only 35 years using the shell parameters. It is clear that the grains will be stopped in only a few hundred years.

Thermal sputtering time of grains with size a can be written as

$$t_{\text{sput}} = a \left[\frac{da}{dt} \right]^{-1} \text{ s} \quad (6)$$

The rate at which the radius of the dust grain changes (da/dt) can be written as a function of the plasma temperature T and number density n_H (Tsai & Mathews 1995):

$$\frac{da}{dt} = -3.2 \times 10^{-18} n_H \left[\left(\frac{2 \times 10^6}{T} \right)^{2.5} + 1 \right]^{-1} \text{ cm s}^{-1} \quad (7)$$

Note that for high temperatures $> 2 \times 10^6 \text{ K}$ characteristic of the bubble interior, this reduces to equation 5. However, the dense shell will have much lower temperatures, on order 10^4 K , with denser regions having even lower temperatures. The sputtering time at these low temperatures increases considerably:

$$t_{\text{sput}} = 5.6 \times 10^{11} \left[\frac{n_H}{\text{cm}^{-3}} \right]^{-1} \left[\frac{a}{1 \mu\text{m}} \right] \left[\frac{T}{10^4 \text{K}} \right]^{-2.5} \text{ yr} \quad (8)$$

The density of the dense shell is higher than the density of the swept-up material around it, and thus could be 10^3 to 10^4 cm^{-3} . Even the high density would give a lifetime against sputtering of order several tens of millions of years, so thermal sputtering becomes irrelevant at this stage due to the low temperatures.

However other processes, such as grain evaporation, and non-thermal sputtering due to high speed collisions between the dust grains and the dense gas, become important during this phase. The relative velocity of the fast grains impacting the dense shell can exceed several hundred km s^{-1} . At these velocities, the grains will experience frictional heating which will raise their temperatures to greater than dust condensation temperatures (Ouellette et al. 2010), which are in the range of 1300-1700 K (Lodders 2003). Thus the impact can cause the grains to vaporize, releasing the ^{26}Al into the dense gas. Non-thermal sputtering, which is independent of the temperature but depends on the relative velocity between the grains and the shell gas, also becomes important at this stage. The rate of non-thermal sputtering is close to its maximum value, and comparable to the value of thermal sputtering, at a relative velocity of about 1000 km s^{-1} (Goodson et al. 2016), which is approximately the value at which the grains impact the dense gas in the shell. Thus at the densities within the shell, the lifetime against sputtering at impact will be on order 1000-10000 years. A fraction of the grains will be sputtered away. As the velocity decreases, this lifetime will increase. Due to frictional drag within the disk (Ouellette et al. 2010) the grains will increase in temperature and some will evaporate.

Estimating what fraction of the grains eventually survive requires numerical simulations taking all the various processes into account, which is beyond the scope of this paper. Simulations under somewhat similar conditions were carried out by Ouellette et al. (2010) and Goodson et al. (2016) for dust grains impacting a dense disk. While the impact velocities and other details differ, the results clearly show that a large fraction of grains $1 \mu\text{m}$ in size will penetrate the dense disk and inject between 40% (Goodson et al. 2016) to 80% (Ouellette et al. 2010) of the SLRs into the dense shell. This is contrasted with direct injection of SLRs by the gas, which was found to be only 1% by Goodson et al. (2016), comparable to the previous results of Boss & Keiser (2013). Ouellette et al. (2010) suggest that up to 40% of the $1 \mu\text{m}$ grains, and about 30% of grains of all sizes, may survive within the dense

disk, although they have not carried their simulations on for much longer to determine whether they will survive or be eventually sputtered or evaporated away. Goodson et al. (2016) estimate that about half of all grains sputter or stop within the cloud, but the velocity of their shock on impact, $\sim 350 \text{ km s}^{-1}$, is smaller than the velocity that the grains in our simulation would have. A larger velocity would increase the amount of non-thermal sputtering.

Using these results as well as our own estimates above, one may expect at least half the ^{26}Al that reaches the dense shell to be injected from the grains to the disk. Even if one assumes that about 20% of the ^{26}Al condenses into dust grains, and half the grains survive within the bubble interior and reach the dense shell, both conservative estimates, we find that a total of $0.2 \times 0.5 \times 0.5 = 0.05$ of the ^{26}Al from the star will reach the dense shell. Thus efficiencies of this order used to calculate the ^{26}Al fraction in section 3.1 were warranted. Furthermore, it appears from the simulations, and assuming the grains are distributed in size around the $1 \mu\text{m}$ value, that at most 1/3 of the grains may eventually survive.

We investigate further if the survival of these grains is consistent with observations of meteorites. Our simulations show that there is extensive mixing in the bubble, so although the ^{26}Al and C may be emitted at somewhat different times, the material can be assumed to be completely mixed in the W-R stage. We therefore consider the bulk composition of the material to determine what the composition of the grains might be. In the models of Ekström et al. (2012), the mass ratio of $^{26}\text{Al}/\text{C}$ in non-rotating stars between initial mass 32 and $120 M_{\odot}$ (the likely mass to form W-R stars) varies between 10^{-3} to $7. \times 10^{-5}$, with stars above $60 M_{\odot}$ having ratios generally a few times 10^{-5} . For rotating stars this ratio lies between 2.6×10^{-5} to $3. \times 10^{-4}$. For simplicity in this calculation we consider a mass ratio 5×10^{-5} .

The mass fraction of ^{26}Al in the initial solar system is given by equation 3 to be 3.25×10^{-9} . If we assume that all the ^{26}Al comes from the W-R star, the fraction of C that then arises from the W-R star, with respect to H and He, is

$$\frac{3.25 \times 10^{-9}}{5 \times 10^{-5}} = 6.5 \times 10^{-5}. \quad (9)$$

What we are really interested in is the mass fraction of C relative to condensable matter found in meteorites, rather than H and He. For the proto-sun, the fraction of metals (essentially everything but H and He) is 0.0149 (Lodders 2003). The main contributors to this are C, N, O, Si, Mg and Fe, with others contributing to a lesser degree. Subtracting species that do not condense such as the rare gases, we find that the mass-fraction of

condensable matter is about 1.3×10^{-2} . Therefore the concentration of C arising from W-R grains, relative to condensable matter, is 5×10^{-3} . If one-third of these grains survived injection into the dense shell and proto-solar system, then the mass-fraction of C grains in the proto-solar system, and thereby in meteorites, would be about 0.16%. This is a large and potentially identifiable fraction.

However, we must also consider that there are processes which destroy dust in the early solar system compared to the dust concentrations in the neighbourhood. [Zhukovska et al. \(2008\)](#) have studied the evolution of various dust species in the ISM at the time of solar system formation. They predict that the mass-fraction of C dust compared to H is about 1500 parts per million (ppm) at time of solar system formation. If one considers dust produced by SNe and AGB stars only, it is a factor of 10 less or about 150 ppm. On the other hand, the mass-fraction of C-containing grains such as graphite and SiC grains found in meteorites is close to 10 ppm ([Nittler 2003](#)). Normalized to H this would be of order 0.1 ppm. This means that there is a destruction factor of order ~ 1000 when going from interstellar dust to dust grains in meteorites. If the same factor was applicable to the W-R grains, this would imply that only 10^{-4} % of the grains would be potentially identifiable in meteorites, a negligible fraction. Thus our assumption of about one-third of the grains surviving does not appear to be a problem from the point of view of meteoritic observations.

The dense shell is clearly not a spherically symmetric, homogeneous shell. It is susceptible to several dynamical and radiative instabilities, such as Vishniac-type thin-shell instabilities, or ionization front instabilities, ([Dwarkadas et al. 1996](#); [Garcia-Segura et al. 1996](#); [Dwarkadas & Balick 1998](#); [Dwarkadas 2007](#); [van Marle & Keppens 2012](#); [Toalá & Arthur 2011](#); [Dwarkadas & Rosenberg 2013](#)) that tend to break up the shell and wrinkle the surface, as seen in [Figure 3](#). The density within the shell is also not completely uniform, since it depends on the surrounding density which may vary over the circumference, the penetration of the ionization front into the shell, and the disruption due to various instabilities. The result is that both the inner radius and density are somewhat variable. The dust grains themselves, although having an average size of $1 \mu\text{m}$, will have a range of sizes around that value. Thus the penetration depth and stopping distance of the dust grains into the dense shell will vary along the circumference of the shell, introducing a level of heterogeneity into the picture of ^{26}Al injection into the collapsing cores.

6. THE SUBSEQUENT SUPERNOVA EXPLOSION

At the end of the W-R stage, the star will end its life in a core-collapse followed by a stellar explosion, giving rise to a supernova shock wave and leaving a compact remnant behind. Some massive stars are predicted to core-collapse all the way to a black-hole, leaving no remnant, and the dividing line is not clearly delineated. In the work of [Georgy et al. \(2012\)](#), stars all the way up to masses of $120 M_{\odot}$ can form a Type Ib/c SN if the formation of a black hole during the process has no influence on the resulting SN explosion. Conversely, if the formation of a black hole does not result in a bright SN explosion, then only stars up to about $34 M_{\odot}$ ($44 M_{\odot}$ in the non-rotating limit) will form Type Ib/c SNe. [Sukhbold & Woosley \(2016\)](#) emphasize that the explosion properties are sensitive to the mass-loss prescription employed. Whether there will be a faint SN, or no SN at all, depends on whether the star can successfully launch an outward moving shock wave (not always the case), and whether there is fallback of the ^{56}Ni into the center ([Woosley et al. 2002](#); [Sukhbold & Woosley 2016](#)). Thus, while it is realistic to assume that W-R stars will form Type Ib/c SNe, up to what initial mass that happens is unclear.

In this work, we have found that we would need a massive star to seed the ^{26}Al in the initial solar system. Depending on the efficiency of mixing ^{26}Al with the surrounding dense shell, in some scenarios we would need a star $> 40 M_{\odot}$. The star either ends its life in a spectacular supernova explosion, or it directly core-collapses into a black hole ([Woosley et al. 2002](#)). If there is no SN explosion then there is no explosive nucleosynthesis, and no resulting shock wave. This will mean that there is no ^{60}Fe produced during the explosion. There is still some ^{60}Fe produced in shell C burning (in stars $< 60 M_{\odot}$) and in shell He burning (in stars $> 60 M_{\odot}$) ([Limongi & Chieffi 2006](#)), which could be ejected, but this material has low velocity and is not pushed by the shock wave into the dense shell. The fraction mixed in with the shell would be considerably reduced from the few percent expected from earlier calculations, to an extremely tiny fraction. Overall we would not expect any significant amount of ^{60}Fe from the fallback SN.

If there is a SN explosion, then explosive nucleosynthesis will take place, accompanied by a shock wave, and there will be production and ejection of ^{60}Fe . In the simulations of [Boss \(2006\)](#); [Foster & Boss \(1997\)](#); [Boss & Keiser \(2013\)](#), it is the transmitted shock into the dense disk, and the associated Rayleigh-Taylor instabilities, that injects SN ejecta into the disk. Therefore this depends crucially on where and how far behind the ^{60}Fe is located in the ejecta. The amount of ^{60}Fe that might be injected to the solar system may be estimated by considering the example of the $40 M_{\odot}$ stellar model in [van Marle et al. \(2005\)](#). By the time the star ends

its life, $31.8 M_{\odot}$ of material is lost via mass-loss to the surrounding medium, which mass is enclosed within the bubble. If $1.5 M_{\odot}$ is assumed to be left behind in a neutron star, the ejected mass will be $6.7 M_{\odot}$. $6.7 M_{\odot}$ sweeping up $31.8 M_{\odot}$ will mean the SN will not have reached the Sedov stage (Dwarkadas & Chevalier 1998), which requires the swept-up mass to be much higher. The expanding shock front will have a double-shocked structure consisting of a forward and reverse shock, separated by a contact discontinuity. Iron-60 can penetrate the dense shell/core if it has already been shocked by the reverse shock and lies near the contact discontinuity which is unstable. For this to happen, the ^{60}Fe must be in the outermost, higher velocity layers which are initially shocked by the reverse shock. Iron-60 is formed in the He or C convective shells, although in stars above $40 M_{\odot}$ the major contribution is from the He burning convective shell (Limongi & Chieffi 2006). One would expect the W-R star to have shed its H, and presumably some portion of its He layer. If ^{60}Fe is mainly formed in the He-shell, then it will lie quite close to the outer edge of the ejecta, and the reverse shock will likely reach it before the forward shock collides with the dense shell. Given that the contact discontinuity is always Rayleigh-Taylor unstable (Chevalier et al. 1992; Dwarkadas 2000) it is possible that parts of the shocked ejecta forming the unstable Rayleigh-Taylor ‘fingers’ that penetrate into the shocked ambient medium, may come into contact with the dense shell/cores. Even then, a further complication is that if the SN forward shock wave has speeds exceeding 1000 km s^{-1} , the post-shock gas will be at temperatures $> 10^7\text{K}$, and will have a difficult time penetrating the colder material, as pointed out earlier (Goswami & Vanhala 2000).

The above arguments assume that the ^{60}Fe is uniformly deposited and the shock wave is spherically symmetric. This is not necessarily the case. W-R stars are also thought to be the progenitors of gamma-ray bursts, where the emission is highly beamed in a jet-like explosion, and thus is highly asymmetric. Although these are the extreme cases, it has been shown, especially from observations of double-peaked profiles in the nebular lines of neutral oxygen and magnesium, that explosions of W-R stars, which lead to Type Ib/c SNe, are generally aspherical (Mazzali et al. 2005). Some results suggest that all supernova explosions from stripped envelope stars have a moderate degree of asphericity (Maeda et al. 2008), with the highest asphericities occurring for SNe linked to gamma-ray bursts. In the current scenario, we can assume that given the small size of the proto-solar nebula compared to the dense shell, even a moderate degree of asphericity such as a factor of 2 would result in a 50% probability that the SN debris, including the ^{60}Fe , would not reach the fledgling solar

system at all.

Therefore we conjecture that there is a high degree of probability that after the death of the W-R star in a core-collapse explosion, the resulting SN ejecta containing ^{60}Fe would not be able to contaminate the proto-solar nebula and raise the level of ^{60}Fe beyond the level of the material in the swept-up dense shell.

The ^{60}Fe within the solar nebula in our model arises in the swept-up material that forms the dense shell. In a steady-state situation, the abundance of ^{60}Fe in the swept-up gas is a result of the Galactic evolution up to the beginning of the solar system, including many past generation of stars. Assuming that the ^{60}Fe had reached an equilibrium situation, the gas should have an abundance of ^{60}Fe equal to the Galactic value as discussed in §1. However, since the star’s lifetime is greater than the lifetime of ^{60}Fe by up to a factor of 2, some of this material will radioactively decay. On average the shell gas will therefore have an ^{60}Fe abundance that is slightly lower than the Galactic value.

7. FORMATION OF THE SOLAR NEBULA:

In our model, the stellar wind reaches the dense shell only after the onset of the W-R phase. After this wind actually reaches the shell, it is decelerated, the dust grains detach from the wind, and are injected into the dense disk, where they are stopped or sputtered away. This process thus takes place in the latter part of the W-R phase, during the WC phase when dust is formed. The lifetime of the WC phase varies from about 1.5×10^5 yr for a $32 M_{\odot}$ star to about 3×10^5 yr for a fast rotating $120 M_{\odot}$ star (Georgy et al. 2012). After the onset of the W-R phase, the wind still takes some time to reach the shell, on order of a few to 10,000 years. The wind is decelerated on impact with the shell but the dust grains detach and continue with the same velocity into the shell. The entire process of the wind being expelled from the star and carrying the dust with it would take less than 2×10^4 yr. We would expect that the timescale for ^{26}Al to be injected and mixed in with the dense shell is less than 10^5 years after ^{26}Al ejection from the star. Uncertainties include how long the dust takes to form, and how long the ^{26}Al takes to condense into the dust grains. Theoretical arguments of the distribution and ages of CAIs in the solar nebula (Ciesla 2010) suggest that the mixing of ^{26}Al with the pre-solar material took place over about 10^5 yr, so our results are consistent with this. During this period of mixing, some portion of the dense shell was collapsing to form molecular cores, including the one that gave rise to our solar system.

The timescale for the triggered star formation is shorter for the radiation-driven implosion mechanism than the collect and collapse mechanism. The average time for fragmentation to start in expanding shells is

of order 0.9 Myr (Whitworth et al. 1994a). Given that the lifetimes of these stars are several million years and the W-R phase occurs only at the end of its life, it is likely that injection of ^{26}Al happens almost simultaneously as the shell is starting to fragment and cores begin to form. Calculations also indicate that heterogeneity in the initial material appears to be preserved as the core collapses (see for e.g. Visser et al. 2009), so we would expect that the ^{26}Al distribution set up by the dust grains will be preserved when parts of the shell collapse to form stars. Since the ^{26}Al does not penetrate all the way into the dense shell, given the short stopping distance, it is likely that there would be some regions which do not contain much or perhaps any ^{26}Al . This is consistent with the fact that FUN CAIs in meteorites show very little to zero ^{26}Al (Esat et al. 1979; Armstrong et al. 1984; MacPherson et al. 2007). Platy hibonite crystals, and related hibonite rich CAIs are not only ^{26}Al poor but appear to have formed with $^{26}\text{Al}/^{27}\text{Al}$ ratio less than the Galactic background (Kööp et al. 2016), whereas spinel hibonite spherules are generally consistent with the canonical $^{26}\text{Al}/^{27}\text{Al}$ ratio (Liu et al. 2009). In the current scenario, such a diversity in ^{26}Al abundance would be expected. In this model our solar system is not the only one with a high ^{26}Al ; other solar systems will be formed over the entire disk area that may also have similar abundances of ^{26}Al . Depending on the subsequent evolution of the star and the formation or not of a SN, these other systems may have different amounts of ^{60}Fe compared to ours. Thus our prediction is that there should be other solar systems with abundance of ^{26}Al similar to ours, but with equal or higher abundances of ^{60}Fe .

8. DISCUSSION AND CONCLUSIONS

The inference of high abundance of ^{26}Al in meteoritic material has led to speculations over several decades that the early solar system formed close to a SN. This however would be accompanied with an abundance of ^{60}Fe above the background level. The recent discovery that the amount of ^{60}Fe in the early solar system was lower than the Galactic background has prompted a re-evaluation of these ideas (Tang & Dauphas 2012).

In this work we have put forward an alternate suggestion, that our solar system was born at the periphery of a Wolf-Rayet bubble. Our model adds details and expands considerably on previous results by Gaidos et al. (2009), Ouellette et al. (2010) and Gounelle & Meynet (2012), while adding some totally new aspects, especially the fact that our solar system was created at the periphery of a Wolf-Rayet wind bubble by triggered star formation. W-R stars are massive stars, generally $\geq 25M_{\odot}$, that form the final post-main-sequence phases of high-mass O and B stars before they core-collapse as super-

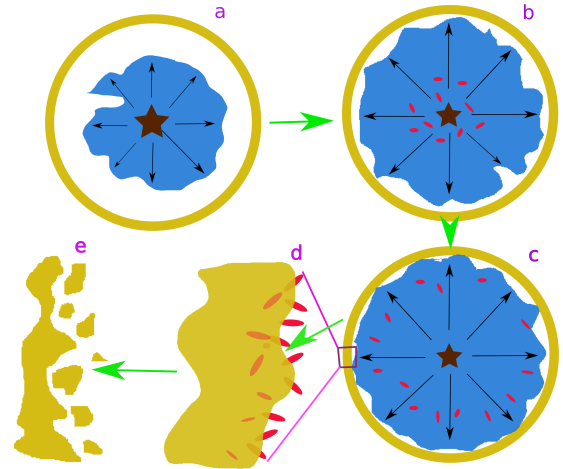


Figure 6. Cartoon version of our model of the formation of the solar system. (a) A massive star forms, and its strong winds and ionizing radiation build a wind-blown bubble. The blue region is the wind-blown region, the yellow is the dense shell. An ionized region (white) separates them. (b) The bubble grows with time as the star evolves into the W-R phase. In this phase, the momentum of the winds pushes the bubble all the way to the shell. At the same time, dust forms in the wind close in to the star, and we assume the ^{26}Al condenses into dust. (c) Dust is carried out by the wind towards the dense shell. (d) The wind is decelerated at the shell but the dust detaches from the wind and continues onward, penetrating the dense shell. (e) Triggered star formation is already underway in the last phase. Eventually some of the material in the shell collapses to form dense molecular cores which will give rise to various solar systems, including ours.

novae (see Figure 6). The ^{26}Al that is formed in earlier phases is carried out by the stellar mass-loss in this phase. The fast supersonic winds from these stars carve out wind-blown bubbles around the star during their lifetime (Figure 6a). These are large low density cavities surrounded by a high-density shell of swept-up material. In our model, the ^{26}Al ejected in the W-R wind (Figure 6b) condenses onto dust grains that are carried out by the wind without suffering much depletion, until they reach the dense shell (Figure 6c). The grains penetrate the shell to various depths depending on the shell density (Figure 6d). The ionization front from the star entering the shell increases the density of the shell, causing material that exceeds a critical mass to collapse and form star-forming cores (Figure 6e). This has been observed at the periphery of many wind bubbles, and we suggest that it is what triggered the formation of our solar system, which was enriched by the ^{26}Al carried out in the W-R wind.

In our model, the ^{26}Al will be injected into the dense shell while the shell material is collapsing to form the dense cores that will form stars that give rise to the solar system. Thus this will happen close to the end of the star's evolution and/or near the SN explo-

sion. Eventually either the SN shock wave will eat away at the bubble and break through it; material will start to leak through the bubble shell, which is generally unstable to various instabilities (Dwarkadas et al. 1996; Garcia-Segura et al. 1996; Dwarkadas & Balick 1998; Dwarkadas 2007; van Marle & Keppens 2012; Toalá & Arthur 2011; Dwarkadas & Rosenberg 2013), until it is completely torn apart; or the bubble shell will dissipate. Either way the nascent solar system will then be free of its confined surroundings.

A single star is responsible for all the ^{26}Al in the initial solar system, and perhaps (see below) for most other short-lived radionuclides (SLRs). Our model uses dust grains as a delivery mechanism for the ^{26}Al into the dense shell that will then collapse to form the pre-solar core. In this our model differs from many previous ones that also suggested W-R stars as the source of the radionuclides. As pointed out, the delivery mechanism and mixing of the SLRs with the presolar molecular cloud is of utmost importance, as also shown by Foster & Boss (1997), Ouellette et al. (2010) and Boss & Keiser (2013); it is very difficult to get tenuous hot gas, whether carried by fast winds or supernova ejecta, to mix with the dense, cold gas in the pre solar molecular cloud. Gounelle & Meynet (2012) considered W-R bubbles, but did not address the crucial part of delivery and mixing of the SLRs into the molecular cloud, attributing it to turbulent mixing. Young (2014) and Young (2016) do consider stellar winds from W-R stars as well as SNe, but did not consider the question of mixing of the wind or SN material with the molecular cloud and the injection of SLRs, simply assuming that it will happen by some unknown mechanism over a relatively long time-period. Gaidos et al. (2009) did address the mixing and also attributed it to dust, and our model is closest in nature to theirs. However, they did not work out a complete and detailed model as we have done here.

Boss & Keiser (2013) conclude that W-R winds are untenable as the source of the ^{26}Al due mainly to 2 reasons: (1) The high wind velocity is not suitable for injection and (2) The wind velocities are too high and will end up destroying the molecular cores rather than triggering star formation. In principle we agree with both of these, and neither of them forms an impediment to our model. We have already mentioned that hydrodynamic mixing due to the wind is not a viable source of mixing, hence our preferred method is via the condensation of ^{26}Al into dust grains, which survive in the low density wind and can be injected into the dense shell. Regarding the fact that the winds will not trigger the star formation, star formation in our model is not triggered by the wind, but by a mechanism that involves the ionization and shock fronts. It should be mentioned that the forward shock of the wind bubble is always radiative, and

is observationally and theoretically measured to move at speeds of $20\text{-}50\text{ km s}^{-1}$. Perhaps the one shortcoming of our model may be that if the molecular cores form too early, they may still be destroyed by the wind. Nonetheless, the eventual proof arises from observations, which clearly show evidence of triggered star formation around numerous wind bubbles, and especially cores undergoing gravitational collapse around a W-R star, as mentioned in §4.

While there is significant circumstantial evidence that triggered star formation occurs at the periphery of wind-blown bubbles, confirmation would require that the age of the subsequently formed stars be much smaller than that of the parent ionizing star. A further question that remains is whether our solar system is in fact special. Whitworth et al. (1994b) have suggested that the collapse of the shocked layers would result in the preferential formation of high mass fragments, although clearly this does not indicate high-mass stars, as each fragment could easily split into several low-mass stars. It is difficult to measure the initial mass function that characterizes the mass-range of the newly formed stars, although some attempts have been made. Zavagno et al. (2006) find about a dozen suspected massive star sources among the possibly hundreds of sources detected in mm and infra-red images of the Galactic HII region RCW79. Deharveng et al. (2006) observe 2 stars with masses $> 10 M_{\odot}$ among about 380 stars expected in a cluster of stars present in the interaction region between the expanding HII region and the molecular cloud in the HII region Sh2-219. Zavagno et al. (2010) find around the HII region RCW120 a single massive star ($8\text{-}10 M_{\odot}$) plus several low mass stars in the range of $0.8\text{-}4 M_{\odot}$. The ages of the low mass stars is about 50,000 years, compared to an age of 2.5 Myr for the parent ionizing star determined from the parent star's photometry and spectral classification (Martins et al. 2010). This suggests that the cluster of low mass stars are coming from a second, presumably triggered generation of stars. One can also appeal to other clusters, not necessarily formed by triggered star formation, that have been studied. Da Rio et al. (2012) have found that the initial mass function (IMF) in the Orion Nebula Cluster is similar to the IMF calculated by Kroupa (2001) and or Chabrier (2003) down to about $0.3 M_{\odot}$, below which it appears to be truncated. Thus, although Whitworth et al. (1994b) may be correct in that there may be some preference towards high-mass stars, it does not appear that there is a significant deviation of the IMF in star-forming regions from the general interstellar IMF. In general, it seems plausible to assume that a solar-mass star is not a special case but may be reasonably expected as a result of triggered star formation.

It is clear that triggered star formation, in bubbles as

well as HII regions, colliding clouds and supernova remnants, is seen. There appears to be a correlation between infrared bubbles and star formation (Kendrew et al. 2012). Many authors (Whitworth et al. 1994a,b; Walch 2014) have suggested that massive stars form via triggered star formation and that this can lead to another generation of triggered stars, leading to so-called sequential star formation. A further question may be whether the formation of a solar mass star via triggering is an unusual circumstance or something that is common. Unfortunately, resolving this requires knowledge of the importance of triggered and sequential star formation versus spontaneous star formation. With a few assumptions, we can make a best case scenario argument as to the probability of a given mass star arising from triggered rather than spontaneous star formation. Let us assume that N stars are born at any given time, out of which N_{WR} stars have a mass $> 25 M_{\odot}$ and go on to form W-R stars, producing a wind-blown bubble with a dense shell. N_G stars have a mass between 0.85 and $1.15 M_{\odot}$ and constitute solar mass stars. The probability that the shell collapses to form stars is β (≤ 1). If it does collapse, N_t stars are formed in the swept-up shell due to triggering. Then the total number of stars formed as a result of triggered star formation in dense shells around W-R stars will be $\beta N_t N_{WR}$. If N_{Gt} solar mass stars are formed due to triggered star formation, then the fraction of solar mass stars in the shell is N_{Gt}/N_t . The total number of solar mass stars formed due to collapse of the shell is then given as $(N_{WR} N_t \beta N_{Gt})/N_t$. The fraction of solar mass stars formed due to triggering, to the total number of solar mass stars formed at any given time, is then $(N_{WR} N_t \beta N_{Gt})/(N_t N_G)$. This can be considerably simplified if we assume that the IMF of the population of triggered stars is the same as that of the population of all newly born stars. In that case $N_{Gt}/N_t = N_G/N$ and the fraction of solar mass stars formed by triggering (F_G) is:

$$F_G = (N_{WR} N_t \beta)/N. \quad (10)$$

We can compute the ratio N_{WR}/N from the initial mass function (IMF). Using the Kroupa IMF, where the number of stars between mass M and $M + dM$ goes as $\xi M = M^{-\alpha} dM$, with $\alpha = 2.3$ for $M > 0.5 M_{\odot}$ and $\alpha = 1.3$ for $0.08 < M < 0.5 M_{\odot}$, the fraction of stars $> 25 M_{\odot}$ is 4.1×10^{-3} . If we assume that gravitational collapse occurs in 10% of the cases ($\beta = 0.1$), and that each triggering episode makes a 100 stars on average, then the fraction of solar mass stars formed by triggering is $4.1 \times 10^{-3} \times 0.1 \times 100 \sim 4\%$ of all stars formed at a given time. The uncertainties include what fraction of the shells actually collapse to form stars, and the total number of stars produced by triggering, or equivalently

the total disk mass that collapses to form stars. Since these numbers are not well calibrated and could vary by a factor of 2 on either end, we estimate conservatively that between 1-16% of solar mass stars could be formed in this manner.

The ratio given in equation 10 above is equally applicable to stars of any given mass, since the stellar mass cancels out. This is due to the assumption that the IMF of triggered star formation is the same as the IMF for all stars. If this were not the case, then we would have in equation 10 an additional factor N_{Gt}/N_G , which basically requires knowing the fraction of solar mass stars due to triggering to the total number of solar mass stars, or equivalently the IMF in each case. We also note here that only wind-blown bubbles around W-R stars are being considered. If we were to take into account bubbles around all main-sequence massive (O and B) stars, the number of stars formed by triggering could be higher, although those stars would not be enriched in ^{26}Al .

Binaries may modify the conclusion above regarding the number of Wolf-Rayet stars, and the number of solar mass stars formed by triggering. It is possible that in a binary, due to more efficient mass transfer or a higher mass-loss rate, the Wolf-Rayet stage could be reached at a lower mass. Georgy et al. (2012) have shown that rotation can also lead to W-R stars forming at a lower mass threshold of about $20 M_{\odot}$.

We have assumed a single central star to be responsible for the ^{26}Al . However as mentioned earlier, dust around W-R stars has been seen predominantly in stars that are binaries. Furthermore massive stars seem to like company - a recent review (Sana 2017) suggested that 50-70% may be in binaries, with some surveys suggesting as high as 90%. Thus it is quite likely that it was not a single star but more likely a W-R star with a companion. These companions are found to usually be other massive O stars. This does not alter our scenario, and possibly enhances the results, because the probability of having sufficient ^{26}Al to pollute the dense shell increases, the expectation of dust formation increases, and the amount of dust formed may be higher.

Can the abundances of other short-lived radionuclides found in the early solar system also be adequately explained by this process? Here we focus on two other species whose early solar system abundances are commonly thought to be possibly due to late incorporation of fresh stellar ejecta, namely, ^{36}Cl and ^{41}Ca . One of the problems in addressing this question is in obtaining the yields of these species. Although Arnould et al. (2006) claim that the abundance of $^{36}\text{Cl}/^{35}\text{Cl}$ carried by the W-R wind is sufficient to produce the value of $^{36}\text{Cl}/^{35}\text{Cl} = 1.4 \pm 0.2 \times 10^{-6}$ observed in the initial solar system, this does not seem obvious from the plots presented in the paper. Both Gaidos et al. (2009) and

Tatischeff et al. (2010) find that using the yields given in the paper, the value is much lower (by orders of magnitude) than the value reported for CAI's. The problem is further compounded by the fact that the initial solar system yield is itself not well calibrated. Most recently, Tang et al. (2017) have calculated the initial solar system value from Curious Marie, an aqueously altered Allende CAI, and found it to be a factor of 10 higher than quoted in Arnould et al. (2006), which would further increase the discrepancy. It is clear that the yields presented in Arnould et al. (2006) would not be able to satisfy this higher value. Other authors (Wasserburg et al. 2011; Lugaro et al. 2012) have similarly suggested that this isotope is unlikely to arise from a stellar pollution scenario. This reinforces the suggestion made previously in the literature, that ^{36}Cl is formed primarily as a result of energetic particle irradiation (Goswami & Vanhala 2000; Wasserburg et al. 2011).

The value of $^{41}\text{Ca}/^{40}\text{Ca}$ for the initial solar system was found by Liu et al. (2012a) to be 4.2×10^{-9} , primarily based on two CAIs from the CV chondrite Efremovka. It appears from the yields given for a 60

M_{\odot} star by Arnould et al. (2006) that this could be easily satisfied in the current model. A crucial question is when exactly the ^{41}Ca was emitted, and how long it took to be injected into the dense shell, given the short half life of 10^5 yr for ^{41}Ca . This requires more information than is available in current stellar evolution models.

We thank the anonymous referee for a comprehensive reading of the manuscript, and for their comments and suggestions which helped to improve this work. This work is supported by a NASA Emerging Worlds program grant # NNX15AH70G awarded to the University of Chicago and a NASA Cosmochemistry grant #NNX14AI25G awarded to Clemson University. VVD would like to thank Prof. Arie H. Konigl for a highly instructive discussion, and for his suggestions. We thank Prof. Georges Meynet for providing their group calculations of the evolution of W-R stars, including the ^{26}Al production.

REFERENCES

- Allen, D. A., Swings, J. P., & Harvey, P. M. 1972, *A&A*, 20, 333
- Armstrong, J. T., Hutcheon, I. D., & Wasserburg, G. J. 1984, in Lunar and Planetary Science Conference, Vol. 15, Lunar and Planetary Science Conference, 15–16
- Arnould, M., Goriely, S., & Meynet, G. 2006, *A&A*, 453, 653
- Arnould, M., Paulus, G., & Meynet, G. 1997, *A&A*, 321, 452
- Biscaro, C., & Cherchneff, I. 2016, *A&A*, 589, A132
- Boehnke, P., McKeegan, K. D., Stephan, T., et al. 2017, in *LPI Contributions*, Vol. 1921, 80th Annual Meeting of the Meteoritical Society, 6456
- Boss, A. P. 2006, *Meteoritics and Planetary Science*, 41, 1695
- Boss, A. P., & Keiser, S. A. 2013, *ApJ*, 770, 51
- Brand, J., Massi, F., Zavagno, A., Deharveng, L., & Lefloch, B. 2011, *A&A*, 527, A62
- Cameron, A. G. W., & Truran, J. W. 1977, *Icarus*, 30, 447
- Cappa, C. E. 2006, in *Revista Mexicana de Astronomia y Astrofisica Conference Series*, Vol. 26, *Revista Mexicana de Astronomia y Astrofisica Conference Series*, 9–12
- Cappa, C. E., Arnal, E. M., Cichowolski, S., Goss, W. M., & Pineault, S. 2003, in *IAU Symposium*, Vol. 212, *A Massive Star Odyssey: From Main Sequence to Supernova*, ed. K. van der Hucht, A. Herrero, & C. Esteban, 596
- Chabrier, G. 2003, *PASP*, 115, 763
- Chevalier, R. A., Blondin, J. M., & Emmering, R. T. 1992, *ApJ*, 392, 118
- Chiar, J. E., & Tielens, A. G. G. M. 2001, *ApJL*, 550, L207
- Ciesla, F. J. 2010, *Icarus*, 208, 455
- Crowther, P. A. 2001, in *Astrophysics and Space Science Library*, Vol. 264, *The Influence of Binaries on Stellar Population Studies*, ed. D. Vanbeveren, 215
- Crowther, P. A. 2007, *ARA&A*, 45, 177
- Da Rio, N., Robberto, M., Hillenbrand, L. A., Henning, T., & Stassun, K. G. 2012, *ApJ*, 748, 14
- Dauphas, N., & Chaussidon, M. 2011, *Annual Review of Earth and Planetary Sciences*, 39, 351
- Deharveng, L., Lefloch, B., Massi, F., et al. 2006, *A&A*, 458, 191
- Deharveng, L., Lefloch, B., Zavagno, A., et al. 2003, *A&A*, 408, L25
- Deharveng, L., Zavagno, A., & Caplan, J. 2005, *A&A*, 433, 565
- Diehl, R., Halloin, H., Kretschmer, K., et al. 2006, *Nature*, 439, 45
- Diehl, R., Lang, M. G., Martin, P., et al. 2010, *A&A*, 522, A51
- Draine, B. T., & Salpeter, E. E. 1979, *ApJ*, 231, 77
- Duprat, J., & Tatischeff, V. 2007, *ApJL*, 671, L69
- Dwarkadas, V. V. 2000, *ApJ*, 541, 418
- Dwarkadas, V. V. 2007, in *Revista Mexicana de Astronomia y Astrofisica Conference Series*, Vol. 30, *Revista Mexicana de Astronomia y Astrofisica Conference Series*, 49–56
- Dwarkadas, V. V., & Balick, B. 1998, *ApJ*, 497, 267
- Dwarkadas, V. V., & Chevalier, R. A. 1998, *ApJ*, 497, 807
- Dwarkadas, V. V., Chevalier, R. A., & Blondin, J. M. 1996, *ApJ*, 457, 773
- Dwarkadas, V. V., & Rosenberg, D. L. 2013, *High Energy Density Physics*, 9, 226
- Ekström, S., Georgy, C., Eggenberger, P., et al. 2012, *A&A*, 537, A146
- Elmegreen, B. G. 2011, in *EAS Publications Series*, Vol. 51, *EAS Publications Series*, ed. C. Charbonnel & T. Montmerle, 45–58
- Elmegreen, B. G., & Lada, C. J. 1977, *ApJ*, 214, 725
- Esat, T. M., Papanastassiou, D. A., & Wasserburg, G. J. 1979, in *Lunar and Planetary Science Conference*, Vol. 10, *Lunar and Planetary Science Conference*, 361–363
- Fedkin, A. V., Meyer, B. S., & Grossman, L. 2010, *GeoCoA*, 74, 3642
- Foster, P. N., & Boss, A. P. 1997, *ApJ*, 489, 346
- Gaidos, E., Krot, A. N., Williams, J. P., & Raymond, S. N. 2009, *ApJ*, 696, 1854
- Garcia-Segura, G., Langer, N., & Mac Low, M.-M. 1996, *A&A*, 316, 133
- Georgy, C., Ekström, S., Meynet, G., et al. 2012, *A&A*, 542, A29
- Georgy, C., Ekström, S., Eggenberger, P., et al. 2013, *A&A*, 558, A103

- Goodson, M. D., Luebbbers, I., Heitsch, F., & Frazer, C. C. 2016, *MNRAS*, 462, 2777
- Goswami, J. N., & Vanhala, H. A. T. 2000, *Protostars and Planets IV*, 963
- Gounelle, M., & Meynet, G. 2012, *A&A*, 545, A4
- Gritschneider, M., Lin, D. N. C., Murray, S. D., Yin, Q.-Z., & Gong, M.-N. 2012, *ApJ*, 745, 22
- Hosokawa, T., & Inutsuka, S.-i. 2005, *ApJ*, 623, 917
- . 2006a, *ApJL*, 648, L131
- . 2006b, *ApJ*, 646, 240
- Huss, G. R., Meyer, B. S., Srinivasan, G., Goswami, J. N., & Sahijpal, S. 2009, *GeoCoA*, 73, 4922
- Iliadis, C., Champagne, A., Chieffi, A., & Limongi, M. 2011, *ApJS*, 193, 16
- Jacobsen, B., Yin, Q.-z., Moynier, F., et al. 2008, *Earth and Planetary Science Letters*, 272, 353
- Kastner, J. H., & Myers, P. C. 1994, *ApJ*, 421, 605
- Kendrew, S., Simpson, R., Bressert, E., et al. 2012, *ApJ*, 755, 71
- Knödseder, J. 1999, *ApJ*, 510, 915
- Kööp, L., Davis, A. M., Nakashima, D., et al. 2016, *GeoCoA*, 189, 70
- Kroupa, P. 2001, *MNRAS*, 322, 231
- Langer, N., Braun, H., & Fliegner, J. 1995, *Ap&SS*, 224, 275
- Lee, T., Papanastassiou, D. A., & Wasserburg, G. J. 1976, *Geophys. Res. Lett.*, 3, 109
- Lefloch, B., & Lazareff, B. 1994, *A&A*, 289, 559
- Limongi, M., & Chieffi, A. 2006, *ApJ*, 647, 483
- Liu, M.-C., Chaussidon, M., Srinivasan, G., & McKeegan, K. D. 2012a, *ApJ*, 761, 137
- Liu, M.-C., McKeegan, K. D., Goswami, J. N., et al. 2009, *GeoCoA*, 73, 5051
- Liu, T., Wu, Y., Zhang, H., & Qin, S.-L. 2012b, *ApJ*, 751, 68
- Lodders, K. 2003, *ApJ*, 591, 1220
- Lugaro, M., Doherty, C. L., Karakas, A. I., et al. 2012, *Meteoritics and Planetary Science*, 47, 1998
- MacPherson, G. J., Bullock, E. S., Janney, P. E., et al. 2007, in *Lunar and Planetary Science Conference*, Vol. 38, Lunar and Planetary Science Conference, 1378
- MacPherson, G. J., Davis, A. M., & Zinner, E. K. 1995, *Meteoritics*, 30, 365
- Maeda, K., Kawabata, K., Mazzali, P. A., et al. 2008, *Science*, 319, 1220
- Marchenko, S. V., & Moffat, A. F. J. 2007, in *Astronomical Society of the Pacific Conference Series*, Vol. 367, *Massive Stars in Interactive Binaries*, ed. N. St.-Louis & A. F. J. Moffat, 213
- Marchenko, S. V., Moffat, A. F. J., Vacca, W. D., Côté, S., & Doyon, R. 2002, *ApJL*, 565, L59
- Marhas, K. K., Goswami, J. N., & Davis, A. M. 2002, *Science*, 298, 2182
- Marhas, K. K., & Mishra, R. K. 2012, *Meteoritics and Planetary Science Supplement*, 75, 5273
- Martin, P., Knödseder, J., Meynet, G., & Diehl, R. 2010, *A&A*, 511, A86
- Martins, F., Pomarès, M., Deharveng, L., Zavagno, A., & Bouret, J. C. 2010, *A&A*, 510, A32
- Mazzali, P. A., Kawabata, K. S., Maeda, K., et al. 2005, *Science*, 308, 1284
- McKee, C. F., van Buren, D., & Lazareff, B. 1984, *ApJL*, 278, L115
- Meyer, B. S., & Clayton, D. D. 2000, *SSRv*, 92, 133
- Mishra, R. K., & Chaussidon, M. 2012, *Meteoritics and Planetary Science Supplement*, 75, 5194
- . 2014, *Earth and Planetary Science Letters*, 398, 90
- Mishra, R. K., & Goswami, J. N. 2014, *GeoCoA*, 132, 440
- Mishra, R. K., Goswami, J. N., Tachibana, S., Huss, G. R., & Rudraswami, N. G. 2010, *ApJL*, 714, L217
- Nittler, L. R. 2003, *Earth and Planetary Science Letters*, 209, 259
- Nozawa, T., Kozasa, T., & Habe, A. 2006, *ApJ*, 648, 435
- Oberlack, U., Diehl, R., Montmerle, T., Prantzos, N., & von Ballmoos, P. 1994, *ApJS*, 92, 433
- Ouellette, N., Desch, S. J., & Hester, J. J. 2007, *ApJ*, 662, 1268
- . 2010, *ApJ*, 711, 597
- Palacios, A., Meynet, G., Vuissoz, C., et al. 2005, *A&A*, 429, 613
- Prantzos, N., & Diehl, R. 1995, *Advances in Space Research*, 15, doi:10.1016/0273-1177(94)00046-4
- . 1996, *PhR*, 267, 1
- Quitté, G., Latkoczy, C., Schönbacher, M., Halliday, A. N., & Günther, D. 2011, *GeoCoA*, 75, 7698
- Quitté, G., Markowski, A., Latkoczy, C., Gabriel, A., & Pack, A. 2010, *ApJ*, 720, 1215
- Ragot, B. R. 2002, *ApJ*, 568, 232
- Rajagopal, J., Menut, J.-L., Wallace, D., et al. 2007, *ApJ*, 671, 2017
- Rightmire, R. A., Simanton, J. R., & Kohman, T. P. 1959, *Physical Review*, 113, 1069
- Samworth, E. A., Warburton, E. K., & Engelbertink, G. A. 1972, *PhRvC*, 5, 138
- Sana, H. 2017, *ArXiv e-prints*, arXiv:1703.01608
- Schaerer, D. 1998, in *Astronomical Society of the Pacific Conference Series*, Vol. 131, *Properties of Hot Luminous Stars*, ed. I. Howarth, 310
- Spitzer, L. 1978, *Physical processes in the interstellar medium*, doi:10.1002/9783527617722
- Sugiura, N., Miyazaki, A., & Yin, Q.-Z. 2006, *Earth, Planets, and Space*, 58, 1079
- Sukhbold, T., & Woosley, S. E. 2016, *ApJL*, 820, L38
- Takigawa, A., Miki, J., Tachibana, S., et al. 2008, *ApJ*, 688, 1382
- Tang, H., & Dauphas, N. 2012, *Earth and Planetary Science Letters*, 359, 248
- . 2015, *ApJ*, 802, 22
- Tang, H., Liu, M. C., McKeegan, K. D., Tissot, F. L. H., & Dauphas, N. 2017, in *Lunar and Planetary Inst. Technical Report*, Vol. 48, *Lunar and Planetary Science Conference*, 2618
- Tatischeff, V., Duprat, J., & de Séréville, N. 2010, *ApJL*, 714, L26
- Telus, M., Huss, G. R., Oglione, R. C., et al. 2016, *GeoCoA*, 178, 87
- Telus, M., Huss, G. R., Oglione, R. C., Nagashima, K., & Tachibana, S. 2012, *Meteoritics and Planetary Science*, 47, 2013
- Toalá, J. A., & Arthur, S. J. 2011, *ApJ*, 737, 100
- Trappitsch, R., Boehnke, P., Stephan, T., et al. 2017, in *LPI Contributions*, Vol. 1921, *80th Annual Meeting of the Meteoritical Society*, 6456
- Tsai, J. C., & Mathews, W. G. 1995, *ApJ*, 448, 84
- Tuthill, P. G., Monnier, J. D., & Danchi, W. C. 1999, *Nature*, 398, 487
- Urey, H. C. 1955, *Proceedings of the National Academy of Science*, 41, 127
- van Marle, A. J., & Keppens, R. 2012, *A&A*, 547, A3
- van Marle, A. J., Langer, N., & García-Segura, G. 2005, *A&A*, 444, 837
- Visser, R., van Dishoeck, E. F., Doty, S. D., & Dullemond, C. P. 2009, *A&A*, 495, 881
- Voss, R., Diehl, R., Vink, J. S., & Hartmann, D. H. 2010, *A&A*, 520, A51
- Voss, R., Martin, P., Diehl, R., et al. 2012, *A&A*, 539, A66
- Walch, S., Whitworth, A. P., Bisbas, T. G., Hubber, D. A., & Wunsch, R. 2015, *MNRAS*, 452, 2794
- Walch, S. K. 2014, in *Astrophysics and Space Science Proceedings*, Vol. 36, *The Labyrinth of Star Formation*, ed. D. Stamatellos, S. Goodwin, & D. Ward-Thompson, 173

- Wang, W., Harris, M. J., Diehl, R., et al. 2007, *A&A*, 469, 1005
- Wasserburg, G. J., Busso, M., Gallino, R., & Nollett, K. M. 2006, *Nuclear Physics A*, 777, 5
- Wasserburg, G. J., Gallino, R., & Busso, M. 1998, *ApJL*, 500, L189
- Wasserburg, G. J., Hutcheon, I. D., Aléon, J., et al. 2011, *GeoCoA*, 75, 4752
- Wasserburg, G. J., Karakas, A. I., & Lugaro, M. 2017, *ApJ*, 836, 126
- Watson, C., Corn, T., Churchwell, E. B., et al. 2009, *ApJ*, 694, 546
- Weaver, R., McCray, R., Castor, J., Shapiro, P., & Moore, R. 1977, *ApJ*, 218, 377
- Weidenschilling, S. J. 1977, *Ap&SS*, 51, 153
- Whitworth, A. P., Bhattal, A. S., Chapman, S. J., Disney, M. J., & Turner, J. A. 1994a, *A&A*, 290, 421
- . 1994b, *MNRAS*, 268, 291
- Williams, P. M. 2002, in *Astronomical Society of the Pacific Conference Series*, Vol. 260, *Interacting Winds from Massive Stars*, ed. A. F. J. Moffat & N. St-Louis, 311
- Williams, P. M., van der Hucht, K. A., & The, P. S. 1987, *A&A*, 182, 91
- Woosley, S. E., Heger, A., & Weaver, T. A. 2002, *Reviews of Modern Physics*, 74, 1015
- Young, E. D. 2014, *Earth and Planetary Science Letters*, 392, 16
- . 2016, *ApJ*, 826, 129
- Zavagno, A., Deharveng, L., Comerón, F., et al. 2006, *A&A*, 446, 171
- Zavagno, A., Pomarès, M., Deharveng, L., et al. 2007, *A&A*, 472, 835
- Zavagno, A., Russeil, D., Motte, F., et al. 2010, *A&A*, 518, L81
- Zhukovska, S., Gail, H.-P., & Trieloff, M. 2008, *A&A*, 479, 453